

**INFLUENCE OF TRANSVERSE ELEMENTS ON THE  
PULLOUT CAPACITY OF METAL STRIP REINFORCEMENT  
IN SANDY SOIL**

**By**

**JAVAD ESFANDIARI**

**Thesis submitted in fulfilment of the requirements  
for the degree of  
Doctor of Philosophy**

**2014**

## DECLARATIONS

I declare that this thesis is the results of my own research, that is does not incorporate without acknowledgment any material submitted for a degree or diploma in any university and does not contain any material previously published, written or produced by another person except where due reference is made in the text.

Signed: \_\_\_\_\_

Candidate's name: Javad Esfandiari

Date:

Signed: \_\_\_\_\_

Supervisor's name: Prof. Dr. Mohammad Razip Selamat

Date:

## ACKNOWLEDGEMENTS

All praises are due to the Creator who reigns over all creations. This thesis is the results of years of work whereby I have been accompanied and supported by many people. It is a pleasant aspect that I have now the opportunity to express my gratitude to all of them.

First and foremost, I would like to express my deepest appreciation to my supervisor Prof. Dr. Mohammad Razip Selamat for the supervision, technical guidance, encouragement, and constant dedication throughout the duration of this research. I owe him a lot of gratitude for having me shown the path of this research. I have learned so many new things from him. Besides being an excellent supervisor, Prof. Dr. Mohammad Razip Selamat was more like a close relative or a good friend to me. I would also like to thank my father and my mother for their prayer and supports. I owe my loving thanks to my wife Sara Esfandiari for supporting me when she has lost a lot due to my research work. Without her encouragement and understanding of me being abroad it would have been impossible for me to finish this research.

During this research I have been helped by many people such as the technicians of geotechnical engineering laboratory Mr. Dziauddin Zainol Abidin and Mr. Muhamad Zabidi Yusuff; of concrete laboratory Mr. Abdullah Md Nanyan and Mr. Mohd. Fouzi Ali; of the School of Mechanical Engineering Mr Baharom Awang, Mohd Sani Sulaiman, and Mohd Shawal Faizal Ismail; and of the School of Material and Mineral Resources Engineering - I wish to extend my warmest thanks to all of them.

## TABLE OF CONTENTS

DECLARATIONS	II
ACKNOELEDGEMENT	III
TABLE OF CONTENTS	IV
LIST OF TABLES	X
LIST OF FIGURES	XII
LIST OF SIMBOLS	XXXI
ABSTRAK	XXLI
ABSTRACT	XXXI

<b>CHAPTER 1 INTRODUCTION</b>	<b>1</b>
1.1 Introduction	1
1.2 Applications in Malaysia and abroad	4
1.3 Recent trends in the use of geosynthetic	6
1.4 Problem Statement	7
1.5 Objectives of the research	8
1.6 Scope of Research	9
1.7 Structure of Thesis	10
<b>CHAPTER 2: LITERATURE REVIEWS</b>	<b>11</b>
2. 1 Introduction	11
2. 2 Pull out and direct shear tests involving reinforcement material	11
2. 3 Effects of boundary conditions	30
2. 4 Standards for pull out box dimensions	33
2. 5 Finite Element Modelling (FEM)	36
2. 6 Theoretical studies (Sawicki, A. (2000))	43
2. 7 Pull out mechanisms of reinforcement (Sawicki, A. (2000))	48
2. 8 Different pull out capacity equations by other researchers	51
2. 9 Application of Buckingham $\pi$ theorem in reinforced soil	55

2. 10 Summary	56
<b>CHAPTER 3: MATERIALS AND METHODS</b>	<b>58</b>
3. 1 Introduction	58
3. 2 Materials for pull out tests	58
3.2. 1.Strips	60
3.2. 2 Longitudinal member	60
3.2. 3 Ribs in place of anchorage elements	63
3.2. 4 Anchorage elements in place of ribs	63
3.2. 5 Stiffeners	65
3.2. 6 Welding work	66
3.2. 7 Galvanized coating on strips.	69
3. 3 Materials for direct shear tests	72
3. 4 Soil used in this study	72
3. 5 Experimental programs	77
3.5. 1 Compaction test	79
3.5.2 Tensile tests	81
3.5.3 Triaxial test	85
3.5.4 Pull out test	89
3.5.5 Direct shear test	98
3. 6 Finite Element modelling with Plaxis software	100
3. 7 Conclusion	101

<b>CHAPTER 4 : RESULTS AND DISCUSSIONS</b>	<b>104</b>
4. 1 Tensile tests	104
4. 2 Pullout test program I	108
4.2. 1 Pullout Test on Plain Strip with $\sigma_n= 50$ kPa, 75 kPa, and 100 kPa	110
4.2. 2 Pullout Test on ribbed Strip on one side with $\sigma_n=50$ kPa, 75 kPa, and 100 kPa	114
4.2. 3 Pullout Test on ribbed Strip on both sides with $\sigma_n=50$ kPa, 75 kPa, and 100 kPa	118
4.2. 4 Pullout Test on Strip with one anchorage element which height was 2 cm and $\sigma_n=50$ kPa, 75 kPa, and 100 kPa	122
4.2. 5 Increase in strip-soil angle of friction with changing strip type	127
4.2. 6 Pullout Test on Strip with one anchorage element which depth was 4 cm and $\sigma_n=50$ kPa, 75 kPa, and 100 kPa	128
4.2. 7 Pullout Test on Strip with one anchorage element which depth was 6 cm and $\sigma_n=50$ kPa, 75 kPa, and 100 kPa	131
4.2. 8 Pullout Test on Strip with one anchorage element which depth was 8 cm and $\sigma_n=50$ kPa, 75 kPa, and 100 kPa	136
4.2. 9 Increase in equivalent strip-soil angle of friction with changing strip	140
4. 3 Pullout test program II	142
4.3. 1 Pullout Test on Strip with 2 anchorage elements ( $n=2$ ) which depth was 2 cm ( $h=2$ cm depth ) and $\sigma_n=50$ kPa, 75 kPa, and 100	146
4.3. 2 Pullout Test on Strip with 2 anchorage elements ( $n=2$ ) which depth was 4 cm ( $h=4$ cm) and $\sigma_n=50$ kPa, 75 kPa, and 100 kPa	150
4.3. 3 Pullout Test on Strip with 2 anchorage elements ( $n=2$ ) which depth was 6 cm ( $h=6$ cm) and $\sigma_n=50$ kPa, 75 kPa, and 100 kPa	154
4.3. 4 Pullout Test on Strip with 2 anchorage elements ( $n=2$ ) which depth was 8 cm ( $h=8$ cm) and $\sigma_n=50$ kPa, 75 kPa, and 100 kPa	158
4.3. 5 Pullout Test on Strip with 3 anchorage elements ( $n=3$ ) which depth was 2 cm ( $h=2$ cm) and $\sigma_n=50$ kPa, 75 kPa, and 100 kPa	164
4.3. 6 Pullout Test on Strip with 3 anchorage elements ( $n=3$ ) which depth was 4 cm ( $h=4$ cm) and $\sigma_n=of 50$ kPa, 75 kPa, and 100 kPa	184
4.3. 7 Pullout Test on Strip with 3 anchorage elements ( $n=3$ ) which depth was 6 cm ( $h=6$ cm) and $\sigma_n=50$ kPa, 75 kPa, and 100 kPa	171
4.3. 8 Pullout Test on Strip with 3 anchorage elements ( $n=3$ ) which depth was 8 cm ( $h=8$ cm) and $\sigma_n=50$ kPa,, 75 kPa, and 100 kPa	175

4.3. 9 Pullout Test on Strip with 4 anchorage elements (n=4) which depth was 2 cm (h=2 cm) and $\sigma_n=50$ kPa, 75 kPa, and 100 kPa	180
4.3. 10 Pullout Test on Strip with 4 anchorage elements (n=4) which depth was 4 cm (h=4 cm) and $\sigma_n=50$ kPa, 75 kPa, and 100 kPa	184
4.3. 11 Pullout Test on Strip with 4 anchorage elements (n=4) which depth was 6 cm (h=6 cm) and $\sigma_n=50$ kPa, 75 kPa, and 100 kPa	188
4.3. 12 Pullout Test on Strip with 4 anchorage elements (n=4) which depth was 8 cm (h=8 cm) and $\sigma_n=50$ kPa, 75 kPa, and 100 kPa	192
4.3. 13 Summary of results from pull out tests involving strips of various counts of anchorage element and of various depths	197
4. 4. Pullout test program III	199
4.4. 1 Pullout Test on Strip with both sides having 1 anchorage element each (n=2), of 2,4, 6 and 8cm (h=2, 4, 6, 8 cm) depth, and $\sigma_n=50$ kPa,	202
4.4. 2 Pullout Test on Strip with both sides having 4 anchorage elements each (n=8), of 2, 4, 6, and 8 cm (h=2,4,6,8 cm) depth, and $\sigma_n=100$ kPa	208
4.4. 3 Pullout Test on Strip with both sides having 2 anchorage elements each (n=4), of 6 cm (h=6 cm) depth, and $\sigma_n=100$ kPa.	212
4. 5 Summary of performance of strips with main geometries	213
4.5. 1 Effect of depth of elements versus pull out capacity	213
4.5. 2 Effect of count of elements versus pull out capacity	217
4.5. 3 Design graphs for practical study in field	221
4. 6 Test program IV	223
4.6. 1 Results from direct shear tests	223
4. 7 Regression analysis on Pullout Tests	229
4. 8 Results of Finite Element Modelling	236
4.8. 1 Finite element modelling of pullout test on plain strip.	237
4.8. 2 Finite element modelling of pullout tests on strips with one anchorage element with depths ranging from 2 cm to 8	240
4.8. 3 Finite element modelling of pullout tests on strips with two anchorage elements with depths ranging from 2 cm to 8 cm	251



4.8. 4 Finite element modelling of pullout tests on strips with three anchorage elements with depths ranging from 2 cm to 8 cm	260
4.8. 5 Finite element modelling of pullout tests on strips with four anchorage elements with depths ranging from 2 cm to 8 cm	270
4.8. 6 . Summary of finite element modelling of pullout tests on strips with none, 1, 2, 3, and 4 anchorage elements, and with depths ranging from 2 cm to 8 cm	280
<b>CHAPTER 5 : CONCLUSIONS AND RECOMMENDATIONS</b>	<b>289</b>
5. 1. Conclusions	289
5. 2. Suggestion for Future Works	291
<b>REFERENCES</b>	<b>292</b>
<b>LIST OF PUBLICATION</b>	<b>305</b>

## LIST OF TABLES

Table 3. 1: Geometry specifications of strips designed for pull out tests	61
Table 3. 2: Minimum required leg length for fillet welding (LANL, 2006)	69
Table 3. 2: Minimum required leg length for fillet welding (LANL, 2006)	71
Table 3. 4: Geometry specifications of plates designed for direct shear tests	74
Table 3. 5. Summary of properties of soil used in the study	78
Table 3. 6: A summary of work carried out in this study	102
Table 4. 1: Results of tensile tests on plain strip	105
Table 4. 2: Pull out test program I	109
Table 4. 3: Pull out test program II	143
Table 4. 4: Pull out test program III	201
Table 4. 5: Pull out test program IV	224
Table 4. 6. A summary of results from direct shear tests	227
Table 4. 7: Modelling data: (a) Summary of model, (b) Coefficients (a) and ANOVA (b), and (c) Coefficients of dimensionless parameter	230
Table 4. 8: Results from various pull out tests and related dimensionless parameters	231
Table 4. 9: Parameters and results from validation tests	233

Table 4. 10: Specifications and results of pull out tests on strips with elements	234
Table 4. 11: Summary of finite element modelling on plain strip	240
Table 4. 12: Summary of modelling strips with one anchorage element	250
Table 4. 13: Summary of modelling strips with two anchorage elements	260
Table 4. 14: Summary of modelling strips with three anchorage elements	269
Table 4. 15: Summary of modelling strips with four anchorage element	279

## LIST OF FIGURES

Figure 1. 1: A profile of commonly installed mechanically reinforced earth	4
Figure 1. 2: A view of MSE from the front showing decorative facing	5
Figure 2. 1: Results from pullout test using geogrid and lightweight aggregate (Bakeer et al., 1998b)	16
Figure 2.2: Results from interface test using geogrid and lightweight aggregate (Bakeer et al., 1998b)	16
Figure 2. 3: Pull out capacity for corrugated strip (Recana et al.,2003)	14
Figure 2. 4: Geogrids used in pull out tests by Alagiyawanna et al., (2001)	17
Figure 2. 5: Result from pullout test for flexible and rigid reinforcement	18
Figure 2. 6: Results from inclined board test and large direct shear box tests involving 60 mm×60 mm geomembrane and geotextile interface	19 19
Figure 2. 7: Strip of different geometres (Recaca et al., 2003)	21
Figure 2. 8: Pullout capacity for horizontal strip (Recana et al., 2003)	
Figure 2. 11: Cases of bearing strength degradation (Palmeira, 2004)	24
Figure 2. 12: Pullout capacity against displacement of steel grid without triangular kinks (Tin et al., 2011)	25
Figure 2. 13: Pullout capacity of steel grid with 1 triangle kink (Tin et al., 2011)	26

Figure 2. 14: Pullout capacity of steel grid with 2 triangle kinks (Tin et al., 2011)	28
Figure 2. 15: Maximum pullout capacities in tests by Tin et al. (2011)	27
Figure 2. 16: Pull out apparatus as used by Abdi and Arjomand (2011)	28
Figure 2. 17: Results of pull out tests by Abdi and Arjomand (2011)	29
Figure 2. 18: Results of tests by Palmeira and Milligan (1989a): (a) influence by rigid or flexible top boundary; (b) influence by wall roughness	30
Figure 2. 19: Pullout interactions for (a) narrow and (b) wide reinforcement	33
Figure 2. 20: FEM of a pull out test by Khedkar and Mandal (2009)	37
Figure 2. 20: FEM of a pull out test by Khedkar and Mandal (2009)	38
Figure 2. 21: Failure zone in modelling by Khedkar and Mandal (2009)	39
Figure 2. 22: Comparison between experimental and FEM results (Duncan and Chang, 1970)	40
Figure 2. 23: Finite element mesh for a pull out test using SAGE CRISP software (Bergado et al., 2003)	41
Figure 2. 24: Results of modelling pull out tests using PLAXIS and SAGE CRISP involving galvanized strip	44
Figure 2.25: Diagrams of: (a) reinforced retaining wall and (b) equilibrium analytical forces associated with the retaining wall (Sawicki, A. (2000)	44
Figure 2. 26: Reinforcement strip model: (a) Reinforcing strip in ‘active’ and ‘resistant’ zones; (b) strip-soil interaction (Sawicki, A. (2000)	45
Figure 2. 27: Equilibrium of forces in reinforcement strip (Sawicki, A. (2000))	46

Figure 2. 28: Failure zone of strip (Sawicki, A. (2000))	49
Figure 2. 29: Active zone of reinforcement (Sawicki, A. (2000))	50
Figure 3. 1: Strips fabricated for this research in lateral view	59
Figure 3. 2: Strips fabricated for this research in longitudinal view	61
Figure 3. 3: The machine used to cut longitudinal member and other parts of a strip	64
Figure 3. 4: Longitudinal member of a strip	64
Figure 3. 5: Strip with ribs on one side	64
Figure 3. 6: Strip with ribs on both sides	65
Figure 3. 7: Anchorage elements in stacks before being attached to longitudinal elements	66
Figure 3. 8: Stiffeners	67
Figure 3. 9: A strip with shearing elements strengthened by stiffeners	68
Figure 3. 10: Strip with shearing elements - 6 cm depth - and stiffeners on both sides	68
Figure 3. 11: Welding work being carried out	70
Figure 3. 12: A galvanizing work in being carried out	72
Figure 3. 13: Anchorage elements being soldered to the main plate by a technician.	73
Figure 3. 14: Specifications of a plate with no element	75
Figure 3. 15: Specifications of a plate with one element	75

Figure 3. 16: Specifications of a plate with two element	76
Figure 3. 17: Galvanized steel plate specifications with three elements	76
Figure 3. 18. Sieve analysis of soil	77
Figure 3. 19: Compaction test equipment	80
Figure 3. 20: Compaction curve for fill soil	80
Figure 3. 21: Tensile test equipment of the School of Civil Engineering, USM	81
Figure 3. 22: Monitoring system of the tensile test equipment	82
Figure 3. 23:Tensile test on plain strip	83
Figure 3. 24: Tensile test on strip with ribs on both side	83
Figure 3. 25: Tensile test on strip with one anchorage element of 6 cm deep	84
Figure 3. 26: Tensile test on strip with two anchorage elements of 6 cm deep	84
Figure 3. 27: The pressured cell of the Triaxial test apparatus	85
Figure 3. 28: Sample wrapped in rubber mounted onto the base of a triaxial cell	86
Figure 3. 29. Wrapped sample being mounted during preparation of a triaxial test	87
Figure 3. 30: Pull out apparatuses used in this study	90
Figure 3. 31. Compaction procedure in pull out box	90

Figure 3. 32: Concrete block connector – strip connection in actual projects	91
Figure 3. 33: Pull rod – strip connection adopted for tests in this study	92
Figure 3. 34: Sleeve in pull out box	92
Figure 3. 35: Front strain gage	93
Figure 3. 36: Rear strain gage	93
Figure 3. 37: Manual for the front strain gage	94
Figure 3. 38: Manual for the rear strain gage	95
Figure 3. 39: Load cell for the pull out apparatuses	95
Figure 3. 40: Data logger for the pull out apparatuses	96
Figure 3. 41: Computer used with the pull out apparatuses	97
Figure 3. 42: Air bag positioned on top of soil in the pull out box	97
Figure 3. 43. Pressure gage for the airbag entrance	99
Figure 3. 44: Pressure gage next to air compressor	99
Figure 3. 45: A Direct shear test apparatus	106
Figure 3. 46: A plate with 3 anchorage elements lying on top of a base of direct shear box	106
Figure 4. 1: Strain versus stress curves for strips	100
Figure 4. 2: Displacement versus force curves for strips	106



Figure 4. 3: Strain versus time curves for strips	106
Figure 4. 4: Front and back displacements versus pull out force for plain strip and $\sigma_n = 50$ kPa	110
Figure 4. 5: Front and back displacements versus time for plain strip and $\sigma_n = 50$ kPa	111
Figure 4. 6: Front and back displacements versus pull out force for plain strip and $\sigma_n = 75$ kPa	111
Figure 4. 7: Front and back displacements versus time for plain strip and $\sigma_n = 75$ kPa	112
Figure 4. 8: Front and back displacements versus pull out force for plain strip and $\sigma_n = 100$ kPa	112
Figure 4. 9: Front and back displacements versus time for plain strip and $\sigma_n =$ kPa	113
Figure 4. 10: Normal force versus pull out force for tests with plain strips	113
Figure 4. 11: Front and back displacements versus pull out force for strip with ribs on one side and $\sigma_n = 50$ kPa	114
Figure 4. 12: Front and back displacements versus time for strip with ribs on one side and $\sigma_n = 50$ kPa	115
Figure 4. 13: Front and back displacements versus pull out force for strip with ribs on one side and $\sigma_n = 75$ kPa	115
Figure 4. 14: Front and back displacements versus time for strip with ribs on one side and $\sigma_n = 75$ kPa	116
Figure 4. 15: Front and back displacements versus pull out force for strip with ribs on one side and $\sigma_n = 100$ kPa	116
Figure 4. 16: Front and back displacements versus time for strip with ribs on one side and $\sigma_n = 100$ kPa	117
Figure 4. 17: Normal force versus pullout force for strip with ribs on one side	117
Figure 4. 18: Force-Displacement curve for ribbed strip on two sides and $\sigma_n = 50$ kPa	118

Figure 4. 19: Time-Displacement curve for ribbed strip on two sides and $\sigma_n = 50$ kPa	119
Figure 4. 20: Force-Displacement curve for ribbed strip on two sides, $\sigma_n = 75$ kPa.	119
Figure 4. 21: Time-Displacement curve for ribbed strip on two sides and $\sigma_n = 75$ kPa	120
Figure 4. 22: Force-Displacement curve for ribbed strip on two sides, $\sigma_n =$ kPa	120
Figure 4. 23: Time-Displacement curve for ribbed strip on two sides, and $\sigma_n = 100$ kPa	121
Figure 4. 24: Normal stresses and pullout force for ribbed strip on two side	121
Figure 4. 25: Force-Displacement curve on strip with $n=1$ , $h= 2$ cm and $\sigma_n =$ kPa	123
Figure 4. 26: Time-Displacement curve on strip with $n=1$ , $h= 2$ cm and $\sigma_n = 50$ kPa	123
Figure 4. 27: Force-Displacement curve on strip with $n=1$ , $h= 2$ cm and $\sigma_n = 75$ kPa	124
Figure 4. 28: Time-Displacement curve on strip with $n=1$ , $h= 2$ cm and $\sigma_n = 75$ kPa	124
Figure 4. 29: Force-Displacement curve on strip with $n=1$ , $h= 2$ cm and $\sigma_n = 100$ kPa	125
Figure 4. 30: Time-Displacement curve on strip with $n=1$ , $h= 2$ cm and $\sigma_n = 100$ kPa	125
Figure 4. 31: Normal stresses and pullout force for strip with $n=1$ and $h=2$ cm	126
Figure 4. 32: Increase in equivalent strip-soil angle of friction with changing strip specification (I)	127
Figure 4. 33: Front and back displacements versus pull out force for strip with one anchorage element of 4 cm depth and $\sigma_n = 50$ kPa	128
Figure 4. 34: Front and back displacements versus time for strip with one anchorage element of 4 cm depth and $\sigma_n = 50$ kPa	129
Figure 4. 35: Front and back displacements versus pull out force for strip with one	129

Figure 4. 36: Front and back displacements versus time for strip with one anchorage element of 4 cm depth and $\sigma_n = 75$ kPa	130
Figure 4. 37: Front and back displacements versus pull out force for strip with one anchorage element of 4 cm depth and $\sigma_n = 100$ kPa	130
Figure 4. 38: Front and back displacements versus pull out force for strip with one anchorage element of 4 cm depth and $\sigma_n = 100$ kPa	131
Figure 4. 39: Normal force versus pullout force for strip with one anchorage element of 4 cm depth	131
Figure 4. 40. Force-Displacement curve on strip with $n=1$ , $h= 6$ cm and $\sigma_n = 50$ kPa	132
Figure 4. 41. Time-Displacement curve on strip with $n=1$ , $h= 6$ cm and $\sigma_n = 50$ kPa	133
Figure 4. 42. Force-Displacement curve on strip with $n=1$ , $h= 6$ cm and $\sigma_n =$ kPa	133
Figure 4. 43. Time-Displacement curve on strip with $n=1$ , $h= 6$ cm and normal stress of 75 kPa	134
Figure 4. 44. Force-Displacement curve on strip with $n=1$ , $h= 6$ cm and $\sigma_n = 100$ kPa	134
Figure 4. 45. Time-Displacement curve on strip with $n=1$ , $h= 6$ cm and $\sigma_n = 100$ kPa	135
Figure 4. 46. Normal stresses and pullout force for strip with $n=1$ and $h=6$ cm depth	135
Figure 4. 47. Force-Displacement curve on strip with $n=1$ , $h= 8$ cm and $\sigma_n = 50$ kPa	137
Figure 4. 48. Time-Displacement curve on strip with $n=1$ , $h= 8$ cm and $\sigma_n = 50$ kPa	137
Figure 4. 49. Force-Displacement curve on strip with $n=1$ , $h= 8$ cm and normal stress of 75 kPa	138
Figure 4. 50. Time-Displacement curve on strip with $n=1$ , $h= 8$ cm and $\sigma_n = 75$ kPa	138
Figure 4. 51. Force-Displacement curve on strip with $n=1$ , $h= 8$ cm and $\sigma_n = 100$ kPa	139

Figure 4. 52. Time-Displacement curve on strip with $n=1$ , $h= 8\text{cm}$ and $\sigma_n = 100$ kPa	139
Figure 4. 53. Normal stresses and pullout force for strip with $n=1$ and $h=8$ cm	140
Figure 4. 54: Increase in equivalent strip-soil angle of friction with changing strip specification (II)	141
Figure 4. 55. Force-Displacement curve on strip with $n=2$ , $h= 2\text{cm}$ and $\sigma_n =50$ kPa	147
Figure 4. 56. Time-Displacement curve on strip with $n=2$ , $h= 2\text{cm}$ and $\sigma_n =50$ kPa	147
Figure 4. 57. Force-Displacement curve on strip with $n=2$ , $h= 2\text{cm}$ and normal stress of 75 kPa	148
Figure 4. 58. Time-Displacement curve on strip with $n=2$ , $h= 2\text{cm}$ and $\sigma_n =50$ kPa	148
Figure 4. 59. Force-Displacement curve on strip with $n=2$ , $h= 2$ cm and normal stress of 100 kPa	149
Figure 4. 60. Time-Displacement curve on strip with $n=2$ , $h= 2\text{cm}$ and $\sigma_n =100$ kPa	149
Figure 4. 61. Force-Displacement curve on strip with $n=2$ , $h= 4$ cm and $\sigma_n =50$ kPa	150
Figure 4. 62. Time-Displacement curve on strip with $n=2$ , $h= 4\text{cm}$ and $\sigma_n = 50$ kPa	151
Figure 4. 63. Force-Displacement curve on strip with $n=2$ , $h= 4$ cm and $\sigma_n =75$ kPa	151
Figure 4. 64. Time-Displacement curve on strip with $n=2$ , $h= 4\text{cm}$ and $\sigma_n =75$ kPa	152
Figure 4. 65. Force-Displacement curve on strip with $n=2$ , $h= 4$ cm and $\sigma_n =100$ kPa	152
Figure 4. 66. Time-Displacement curve on strip with $n=2$ , $h= 4\text{cm}$ and $\sigma_n =100$ kPa	153
Figure 4. 67. Normal stresses versus pullout force for strip with $n=2$ and $h=4$ cm	154
Figure 4. 68. Force-Displacement curve on strip with $n=2$ , $h= 6$ cm and normal stress of 50 kPa	155

Figure 4. 69. Time-Displacement curve on strip with $n=2$ , $h= 6$ cm and $\sigma_n = 50$ kPa	155
Figure 4. 70. Force-Displacement curve on strip with $n=2$ , $h= 6$ cm and $\sigma_n =75$ kPa	156
Figure 4. 71. Time-Displacement curve on strip with $n=2$ , $h= 6$ cm and $\sigma_n =75$ kPa	156
Figure 4. 72. Displacement curve on strip with $n=2$ , $h= 6$ cm and $\sigma_n = 100$ kPa	157
Figure 4. 73. Time-Displacement curve on strip with $n=2$ , $h= 6$ cm and $\sigma_n =10$ kPa	157
Figure 4. 74. Normal stresses and pullout force for strip with $n=2$ and $h=6$ cm	158
Figure 4. 75. Displacement curve on strip with $n=2$ , $h= 8$ cm and $\sigma_n =50$ kPa	159
Figure 4. 76. Time-Displacement curve on strip with $n=2$ , $h= 8$ cm and $\sigma_n = 50$ kPa	160
Figure 4. 77. Displacement curve on strip with $n=2$ , $h= 8$ cm and $\sigma_n =75$ kPa	160
Figure 4. 78. Time-Displacement curve on strip with $n=2$ , $h= 8$ cm and $\sigma_n =75$ kPa	161
Figure 4. 79. Displacement curve on strip with $n=2$ , $h= 8$ cm and $\sigma_n =100$ kPa	161
Figure 4. 80. Time-Displacement curve on strip with $n=2$ , $h= 8$ cm and $\sigma_n =100$ kPa	162
Figure 4. 81. Normal stresses and pullout force for strip with $n=2$ and $h=8$ cm	162
Figure 4. 82: Increase in equivalent strip-soil angle of friction with changing strip specification (III)	163
Figure 4. 83. Displacement curve on strip with $n=3$ , $h= 2$ cm and $\sigma_n =50$ kPa	164
Figure 4. 84. Time-Displacement curve on strip with $n=3$ , $h= 2$ cm and normal stress of $50$ kPa	165

Figure 4. 85. Displacement curve on strip with $n=3$ , $h= 2$ cm and $\sigma_n =75$ kPa	165
Figure 4. 86. Time-Displacement curve on strip with $n=3$ , $h= 2$ cm and normal stress of 75 kPa	166
Figure 4. 87. Displacement curve on strip with $n=3$ , $h= 2$ cm and $\sigma_n =100$ kPa	166
Figure 4. 88. Time-Displacement curve on strip with $n=3$ , $h= 2$ cm and $\sigma_n = 100$ kPa	167
Figure 4. 89. Normal stresses versus pullout force for strip with $n=3$ and $h=2$ cm	167
Figure 4. 90. Displacement curve on strip with $n=3$ , $h= 4$ cm and $\sigma_n =50$ kPa	168
Figure 4. 91. Time-Displacement curve on strip with $n=3$ , $h= 4$ cm and normal stress of 50 kPa	169
Figure 4. 92. Displacement curve on strip with $n=3$ , $h= 4$ cm and $\sigma_n =75$ kPa	169
Figure 4. 93. Time-Displacement curve on strip with $n=3$ , $h= 4$ cm and $\sigma_n =75$ kPa	170
Figure 4. 94: Displacement curve on strip with $n=3$ , $h= 4$ cm and normal stress of 100 kPa	170
Figure 4. 95. Time-Displacement curve on strip with $n=3$ , $h= 4$ cm and $\sigma_n =100$ kPa	171
Figure 4. 96. Normal stresses and pullout force for strip with $n=3$ and $h=4$ cm	171
Figure 4. 97. Displacement curve on strip with $n=3$ , $h= 6$ cm and $\sigma_n =50$ kPa	172
Figure 4. 98. Time-Displacement curve on strip with $n=3$ , $h= 6$ cm and $\sigma_n =50$ kPa	173
Figure 4. 99. Displacement curve on strip with $n=3$ , $h= 6$ cm and $\sigma_n =75$ kPa	173
Figure 4. 100. Time-Displacement curve on strip with $n=3$ , $h= 6$ cm and $\sigma_n = 75$ kPa	174
Figure 4. 101. Displacement curve on strip with $n=3$ , $h= 6$ cm and $\sigma_n = 100$ kPa	174

Figure 4. 102. Time-Displacement curve on strip with $n=3$ , $h= 6$ cm and normal stress of 100 kPa	175
Figure 4. 103. Normal stresses and pullout force for strip with $n=3$ and $h=6$ cm	175
Figure 4. 104. Displacement curve on strip with $n=3$ , $h= 8$ cm and $\sigma_n = 50$ kPa	176
Figure 4. 105. Time-Displacement curve on strip with $n=3$ , $h= 8$ cm and $\sigma_n = 5$ kPa	177
Figure 4. 106. Displacement curve on strip with $n=3$ , $h= 8$ cm and $\sigma_n =75$ kPa	177
Figure 4. 107. Time-Displacement curve on strip with $n=3$ , $h= 8$ cm and $\sigma_n =7$ kPa	178
Figure 4. 108. Displacement curve on strip with $n=3$ , $h= 8$ cm and $\sigma_n =100$ kPa	178
Figure 4. 109. Time-Displacement curve on strip with $n=3$ , $h= 8$ cm and $\sigma_n =1$ kPa	179
Figure 4. 110. Normal stresses and pullout force for strip with $n=3$ and $h=8$ cm	179
Figure 4. 111: Increase in equivalent strip-soil angle of friction with changing strip specification (IV)	180
Figure 4. 112. Displacement curve on strip with $n=4$ , $h= 2$ cm and $\sigma_n = 50$ kPa	181
Figure 4. 113. Time-Displacement curve on strip with $n=4$ , $h= 2$ cm and normal stress of 50 kPa	181
Figure 4. 114. Displacement curve on strip with $n=4$ , $h= 2$ cm and $\sigma_n =75$ kPa	182
Figure 4. 115: Time-Displacement curve on strip with $n=4$ , $h= 2$ cm and $\sigma_n =7$ kPa	182
Figure 4. 116. Displacement curve on strip with $n=4$ , $h= 2$ cm and $\sigma_n =100$ kPa	183
Figure 4. 117. Displacement curve on strip with $n=4$ , $h= 2$ cm and $\sigma_n =100$ kPa	183

Figure 4. 118. Normal stresses versus pullout force for strip with $n=4$ and $h=2$ cm	184
Figure 4. 119. Displacement curve on strip with $n=4$ , $h= 4$ cm and $\sigma_n =50$ kPa	185
Figure 4. 120. Displacement curve on strip with $n=4$ , $h= 4$ cm and $\sigma_n =50$ kPa	185
Figure 4. 121. Displacement curve on strip with $n=4$ , $h= 4$ cm and $\sigma_n = 75$ kPa	186
Figure 4. 122. Displacement curve on strip with $n=4$ , $h= 4$ cm and $\sigma_n =75$ kPa	186
Figure 4. 123. Displacement curve on strip with $n=4$ , $h= 4$ cm and normal stress of 100 kPa	187
Figure 4. 124. Displacement curve on strip with $n=4$ , $h= 4$ cm and $\sigma_n = 100$ kPa	187
Figure 4. 125. Normal stresses versus pullout force for strip with $n=4$ and $h=4$ cm	188
Figure 4. 126. Displacement curve on strip with $n=4$ , $h= 6$ cm and $\sigma_n =50$ kPa	189
Figure 4. 127. Displacement curve on strip with $n=4$ , $h= 6$ cm and $\sigma_n =50$ kPa	189
Figure 4. 128. Displacement curve on strip with $n=4$ , $h= 6$ cm and normal stress of 75 kPa	190
Figure 4. 129. Displacement curve on strip with $n=4$ , $h= 6$ cm and $\sigma_n =75$ kPa	190
Figure 4. 130. Displacement curve on strip with $n=4$ , $h= 6$ cm and normal stress of 100 kPa	191
Figure 4. 131. Displacement curve on strip with $n=4$ , $h= 6$ cm and $\sigma_n =100$ kPa	191
Figure 4. 132. Normal stresses versus pullout force for strip with $n=4$ and $h=6$ cm	192
Figure 4. 133. Displacement curve on strip with $n=4$ , $h= 8$ cm and $\sigma_n =50$ kPa	193
Figure 4. 134. Displacement curve on strip with $n=4$ , $h= 8$ cm and $\sigma_n =75$ kPa	193



Figure 4. 135. Displacement curve on strip with $n=4$ , $h= 8$ cm and $\sigma_n = 100$ kPa	194
Figure 4. 136. Displacement curve on strip with $n=4$ , $h= 8$ cm and $\sigma_n = 50$ kPa	194
Figure 4. 137. Displacement curve on strip with $n=4$ , $h= 8$ cm and $\sigma_n =750$ kPa	195
Figure 4. 138. Displacement curve on strip with $n=4$ , $h= 8$ cm and $\sigma_n =100$ kPa	195
Figure 4. 139. Normal stresses versus pullout force for strip with $n=4$ and $h=8$ cm..	196
Figure 4. 140: Increase in equivalent strip-soil angle of friction with changing strip specification (V	196
Figure 4. 141: A comparison of results from various test series (a) Plain strip, strip with ribs on one side, strip with ribs on both sides, and strip with one anchorage elements (b) strip with 2 anchorage elements (c) strip with 3 anchorage elements and (d) strip with 4 anchorage elements	198
Figure 4. 142: Front and back displacements versus pull out force for strip with top and bottom anchorage elements of 2 cm depth ( $n=2$ , $h=2$ cm) and $\sigma_n =50$ kPa	203
Figure 4. 143: Front and back displacements versus time for strip with top and bottom anchorage elements of 2 cm depth ( $n=2$ , $h=2$ cm) and $\sigma_n = 50$ kPa	203
Figure 4. 144: Front and back displacements versus pull out force for strip with top and bottom anchorage elements of 4 cm depth ( $n=2$ , $h=4$ cm) and $\sigma_n =50$ kPa	204
Figure 4. 145: Front and back displacements versus time for strip with top and bottom anchorage elements of 4 cm depth ( $n=2$ , $h=4$ cm) and $\sigma_n =50$ kPa	204
Figure 4. 146: Front and back displacements versus pull out force for strip with top and bottom anchorage elements of 6 cm depth ( $n=2$ , $h=6$ cm) and $\sigma_n =50$ kPa	205
Figure 4. 147: Front and back displacements versus time for strip with top	205

Figure 4. 148: Front and back displacements versus pull out force for strip with top and bottom anchorage elements of 6 cm depth (n=2, h=8 cm) and $\sigma_n = 50$ kPa	
Figure 4. 149: Front and back displacements versus time for strip with top and bottom anchorage elements of 6 cm depth (n=2, h=8 cm) and $\sigma_n = 50$ kPa	206
Figure 4. 150: Strip specification versus pull out capacity for strip with 2 anchorage elements (a) an anchorage element attached to top of strip and another at the bottom (b) both anchorage elements attached at the bottom	207
Figure 4. 151: Front and back displacements versus pull out force with elements of 2, 4, 6, and 8 cm depths attached to top and bottom of a strip (n=8, h=2,4,6, and 8 cm) and $\sigma_n = 100$ kPa	209
Figure 4. 152: Front and back displacements versus time with elements of 2, 4, 6, and 8 cm depths attached to top and bottom of a strip (n=8, h=2,4,6, and 8 cm) and $\sigma_n = 100$ kPa	209
Figure 4. 153: Strip specification versus pull out capacity for strip with various arrangements involving anchorage elements	210
Figure 4. 154: Front and back displacements versus pull out force with elements of 6 cm depths 2 attached to the top and 2 at the bottom of a strip (n=4, h=6 cm) and $\sigma_n = 100$ kPa	211
Figure 4. 155: Front and back displacements versus time with elements of 6 cm depths, 2 attached to the top and 2 at the bottom of a strip (n=4, h=6 cm) and $\sigma_n = 100$ kPa	212
Figure 4. 156: Strip specification versus pull out capacity for strip with various arrangements involving anchorage elements	212
Figure 4. 157. Performances of ribbed and plain strips	214
Figure 4. 158: Performance of Strips with 1 element	215
Figure 4. 159. Performance of Strips with 2 elements	215

Figure 4. 160. Performance of Strips with 3 elements	216
Figure 4. 161. Performance of Strips with 4 elements	216
Figure 4. 162: Performance of Strips with h=2 cm	217
Figure 4. 163. Performance of Strips with h=4cm	218
Figure 4. 164: Performance of Strips with h=6 cm	218
Figure 4. 165: Performance of Strips with h=8 cm	219
Figure 4. 166: Photo showing plastic deformation involving strip with extra long anchorage element	220
Figure 4. 167: Effect of count divided by depth of elements on pull out capacity	231
Figure 4. 168: Relative change in pull out capacity with increasing height and count of elements	222
Figure 4. 169: Displacement versus shearing stress involving one shear element of various heights - $\sigma = 40$ kPa	225
Figure 4. 170: Displacement versus shearing stress involving 2 shear elements of various heights - $\sigma = 40$ kPa	226
Figure 4. 171: Displacement versus shearing stress involving three shear elements of various heights - $\sigma = 40$ kPa	226
Figure 4. 172: Effects of height of element on equivalent friction angel of various counts of elements	228
Figure 4. 173: Stress- strain curve from triaxial test	228
Figure 4. 174: Comparison of (F/P) Experimental and (F/P)Predicted	236
Figure 4. 175: Zones of horizontal displacement surrounding a plain strip under pull out loading	238

Figure 4. 176: Shear stress zones surrounding a plain strip under pull out loading	238
Figure 4. 177: Deformed mesh surrounding a plain strip under maximum pull out loading corresponding to maximum displacement of 10.37 mm	239
Figure 4. 178: Stress points showing principal stresses surrounding a plain strip under pull out loading	239
Figure 4. 179: Zones of displacement surrounding a strip with an anchorage element of 2 cm deep under pull out loading	241
Figure 4. 180: Stress zones surrounding a strip with an anchorage element of 2 cm deep under pull out loading	242
Figure 4. 181: Deformed mesh surrounding a strip with 2 cm deep anchorage element under pull out loading	242
Figure 4. 182: Stress points showing principal stresses surrounding a strip with 2 cm anchorage element under pull out loading	243
Figure 4. 183: Zones of displacement surrounding a strip with an anchorage element of 4 cm deep under pull out loading	243
Figure 4. 184: Stress zones surrounding a strip with an anchorage element of 4 cm deep under pull out loading	244
Figure 4. 185: Deformed mesh of strip with one anchorage element and 4 cm height under maximum pullout force	244
Figure 4. 186: Stress points showing principal stresses surrounding a strip with 4 cm anchorage element under pull out loading	245
Figure 4. 187: Zones of displacement surrounding a strip with an anchorage element of 6 cm deep under pull out loading	245
Figure 4. 188: Stress zones surrounding a strip with an anchorage element of 6 cm deep under pull out loading	246
Figure 4. 189: Deformed mesh of strip with one anchorage element and 6 cm height under maximum pullout force	246
Figure 4. 190: Stress points showing principal stresses surrounding a strip with 6 cm anchorage element under pull out loading	247
Figure 4. 191: Zones of displacement surrounding a strip with an anchorage element of 8 cm deep under pull out loading	247
Figure 4. 192: Stress zones surrounding a strip with an anchorage element of 8 cm	248

Figure 4. 193: Deformed mesh surrounding a strip with 8 cm deep anchorage element under pull out loading	248
Figure 4. 194: Stress points showing principal stresses surrounding a strip with 8 cm anchorage element under pull out loading	249
Figure 4. 195: Zones of displacement surrounding a strip with 2 anchorage elements of 2 cm deep under pull out loading	252
Figure 4. 196: Stress zones surrounding a strip with 2 anchorage elements of 2 cm deep under pull out loading	252
Figure 4. 197. Deformed mesh surrounding a strip with 2 anchorage elements of 2 cm depth under pull out loading	253
Figure 4. 198: Stress points showing principal stresses surrounding a strip with 2 anchorage elements of 2 cm depth under pull out loading	253
Figure 4. 199. Zones of displacement surrounding a strip with 2 anchorage elements of 4 cm deep under pull out loading	254
Figure 4. 200. Stress zones surrounding a strip with 2 anchorage elements of 4 cm deep under pull out loading	254
Figure 4. 201. Deformed mesh surrounding a strip with 2 anchorage elements of 4 cm depth under pull out loading	255
Figure 4. 202: Stress points showing principal stresses surrounding a strip with 2 anchorage elements of 4 cm depth under pull out loading	255
Figure 4. 203. Zones of displacement surrounding a strip with 2 anchorage elements of 6 cm deep under pull out loading	256
Figure 4. 204. Stress zones surrounding a strip with 2 anchorage elements of 6 cm deep under pull out loading	256
Figure 4. 205. Deformed mesh surrounding a strip with 2 anchorage elements of 6 cm depth under pull out loading	257
Figure 4. 207: Zones of displacement surrounding a strip with 2 anchorage elements of 8 cm deep under pull out loading	258
Figure 4. 208: Stress zones surrounding a strip with 2 anchorage elements of 8 cm deep under pull out loading	258
Figure 4. 209: Deformed mesh surrounding a strip with 2 anchorage elements of 8 cm depth under pull out loading	259

Figure 4. 210: Stress points showing principal stresses surrounding a strip with 2 anchorage elements of 8 cm depth under pull out loading	259
Figure 4. 211: Failure zone of strip with three anchorage element and 2 cm height under pull out force in horizontal direction	261
Figure 4. 212: Failure zone in x-y direction of pull out force in strip with three anchorage element and 2 cm height	261
Figure 4. 213: Deformed mesh of strip with tow anchorage element and 2 cm height under maximum pullout force	262
Figure 4. 214: Stress point in pullout box under over pressure and pull out force	262
Figure 4. 214: Stress point in pullout box under over pressure and pull out force	263
Figure 4. 215: Failure zone of strip with three anchorage element and 4 cm height under pull out force in horizontal direction	263
Figure 4. 215: Failure zone of strip with three anchorage element and 4 cm height under pull out force in horizontal direction	264
Figure 4. 216: Failure zone in x-y direction of pull out force in strip with three anchorage element and 4 cm height	264
Figure 4. 217: Deformed mesh of strip with tow anchorage element and 4 cm height under maximum pullout force	265
Figure 4. 218: Stress point in pullout box under over pressure and pull out force	265
Figure 4. 219: Failure zone of strip with three anchorage element and 6 cm height under pull out force in horizontal direction	266
Figure 4. 220: Failure zone in x-y direction of pull out force in strip with three anchorage element and 4 cm height	267
Figure 4. 221: Deformed mesh of strip with tow anchorage element and 6 cm height under maximum pullout force	267
Figure 4. 222: Stress point in pullout box under over pressure and pull out force	268
Figure 4. 223: Failure zone of strip with three anchorage element and 8 cm height under pull out force in horizontal direction	268
Figure 4. 224: Failure zone in x-y direction of pull out force in strip with three	271

anchorage element and 8 cm height	
Figure 4. 225: Deformed mesh of strip with tow anchorage element and 6 cm height under maximum pullout force	271
Figure 4. 226: Stress point in pullout box under over pressure and pull out force	272
Figure 4. 227. Failure zone of strip with four anchorage element and 2 cm height under pull out force in horizontal direction	272
Figure 4. 228. Failure zone in x-y direction of pull out force in strip with four anchorage element and 2 cm height	273
Figure 4. 229. Deformed mesh of strip with four anchorage element and 4 cm height under maximum pullout force	272
Figure 4. 230. Stress point in pullout box under over pressure and pull out force	272
Figure 4. 231. Failure zone of strip with four anchorage element and 6 cm height under pull out force in horizontal direction	273
Figure 4. 231. Failure zone of strip with four anchorage element and 6 cm height under pull out force in horizontal direction	273
Figure 4. 232. Failure zone in x-y direction of pull out force in strip with four anchorage element and 4 cm height	273
Figure 4. 233. Deformed mesh of strip with four anchorage element and 4 cm height under maximum pullout force	274
Figure 4. 234. Stress point in pullout box under over pressure and pull out force	274
Figure 4. 235. Failure zone of strip with four anchorage element and 6 cm height under pull out force in horizontal direction	275
Figure 4. 236. Failure zone in x-y direction of pull out force in strip with four anchorage element and 6 cm height	275
Figure 4. 237. Deformed mesh of strip with four anchorage element and 6 cm height under maximum pullout force	276
Figure 4. 238. Stress point in pullout box under over pressure and pull out force	276
Figure 4. 239. Failure zone of strip with four anchorage element and 8 cm height under pull out force in horizontal direction	277

Figure 4. 240. Failure zone in x-y direction of pull out force in strip with four anchorage element and 8 cm height	277
Figure 4. 241. Deformed mesh of strip with four anchorage element and 8 cm height under maximum pullout force	278
Figure 4. 242. Stress point in pullout box under over pressure and pull out force	278
Figure 4.243: Maximum horizontal displacement versus maximum shear stress	282
Figure 4.244: Maximum horizontal displacement versus maximum shear stress	283
Figure 4.245: Redistribution of stressed regions by changing count of anchorage elements (a) no anchorage element (b) one anchorage element (c) 2 anchorage element (d) 3 anchorage elements (e) 4 anchorage elements	284
Figure 4.246: Redistribution of stressed regions by changing count of anchorage elements (a) no anchorage element (b) one anchorage element (c) 2 anchorage element (d) 3 anchorage elements (e) 4 anchorage elements	286
Figure 4.247: Redistribution of stressed regions by changing count of anchorage elements (a) no anchorage element (b) one anchorage element (c) 2 anchorage element (d) 3 anchorage elements (e) 4 anchorage elements	287



## LIST OF SYMBOL

$PR_s$  = Pull out capacity of skin friction in reinforcement

$PR_b$  = Pull out capacity of transverse ribs in reinforcement

$\alpha_s$  = Fraction of reinforcement surface which is solid

$LR$  = Length of specimen

$\sigma_n$  = Normal stress

$\delta$  = Interface friction angle

$S$  = Distance between transverse members

$\alpha\beta$  = Fraction of total frontal area of reinforcement available for bearing

$h$  = Depth of anchorage element

$n$  = Count of anchorage element

$\sigma_b$  = Passive bearing of transverse member in soil

$fb$  = Pull out interaction of soil-reinforcement

$\phi$  = Friction angle of soil

$Nt = \left(\frac{LR}{S}\right)$  = Length divided to distance of transverse member

$Ntb$  = node number in transverse elements

$Ab$  = area of each rib element (single node and bar between two nodes)

$Nq$  = Bearing resistance factor for transverse members

$F_1$  = "Ultimate frictional of all longitudinal ribs"

$F_2$  = "Ultimate frictional resistance of all transverse ribs"

$F_3$  = "ultimate bearing resistance of all transverse ribs"

$A_l$  = surface of longitudinal members

$A_t$  = surface of transverse ribs

$A_b$  = bearing surface of ribs

$f$  = Pull out resistance factor

$\alpha$  = correction coefficient of nonlinear shear stress distribution on reinforcement

( $\alpha = 1$  for metal strip)

$\sigma_n$  = Vertical normal stress

$Le$  = Effective length of strip

$B$  = Weight of strip

$C$  = Effective unit of perimeter on strip

**$f$  = adherence coefficient of soil – geogrid**

**$\alpha$  = scale correction factor**

$e$  = thickness of transverse rib

s = transverse ribs spacing

$\alpha s$  = ratio between the plane area of geogrids (transverse and longitudinal)

$\alpha p$  = " Ratio between transverse element where in passive resistance is fully moved and corresponding total area"

$\frac{\phi_s}{GGR}$  = soil-geogrids friction angle

M = Mass

L = length

T = time

$\tau_{max}$  = maximum shearing force

$\sigma_n$  = normal stress

$D_{10}$  = Particle diameter soil size that 10 % passing

$D_{30}$  = Particle diameter soil size that 30 % passing

$D_{50}$  = Particle diameter soil size that 50 % passing

$D_{60}$  = Particle diameter soil size that 60 % passing

$G_s$  = Specific gravity

$e_{min}$  = Minimum void ratio

$e_{max}$  = Maximum void ratio

USCS Classification = unified soil classification system

$\gamma_d$  = Maximum Dry Unit Weight

w = Optimum moisture content

$C_u$  = Coefficient of Uniformity

$C_c$  = Coefficient of Curvature

$\phi$  = Angle of Friction

$D_r$  = Relative density of soil

$\Psi$  = Dilatancy angle of soil

## **KAJIAN KESAN UNSUR SAUH KEATAS KEKUATAN TARIK KELUAR JALUR TETULANG DALAM PASIR**

### **ABSTRAK**

Sudut ricih permukaan di antara dua jenis bahan suatu parameter yang sangat penting dalam rekabentuk tanah terstabil mekanikal (MSE) kerana ianya berkait terus dengan keupayaan rintangan tarik keluar jalur pengukuh. Dalam penyelidikan ini, anggota sauh telah ditambah keatas jalur pengukuh bagi meningkatkan sudut ricih permukaan dan keupayaan rintangan tarik keluar. Pasir digunakan sebagai bahan isi. Dalam ujian yang dijalankan, satu jalur licin, dua jalur dengan rasuk mudah, dan lapan belas jalur beranggota melintang dengan berbagai kedalaman dan bilangan telah dikenakan beban tarik keluar dengan tegasan pugak berjulat 50 kPa hingga 100 kPa. Teorem  $\pi$ -Buchingham dan analisis regresi menggunakan perisian statistik – SPSS v.14 – telah juga digunakan bagi menentukan persamaan am yang mengaitkan antara keupayaan rintangan tarik keluar dengan parameter jalur, dan membandingkan diantara kekuatan anggaran dengan keputusan sebenar ujian. Hasil kajian mendapati bahawa kaedah baru melibatkan anggota sauh boleh memberi penjimatan penggunaan jalur atau rekabentuk MSE tertentu yang sesuai digunakan bagi ruangan sempit, lantaran peningkatan rintangan tarik keluar bagi setiap jalur boleh mengurangkan panjang keseluruhan atau jumlah bahan yang diperlukan dalam setiap projek. Dalam kajian ini juga, radas ujian rich terus telah digunakan bagi menentukan rintangan ricih permukaan diantara sampel pamsir terged baik dengan

plat keluli tergalvani. Akhir sekali, pemodelan unsur terhingga telah dijalankan bagi melengkapkan analisis. Keputusan ujian tarik keluar yang digabungkan dengan keputusan pemodelan didapati sangat berguna bagi jurutera menentukan rekabentuk terbaik struktur tanah terkukuh.

# **INFLUENCE OF TRANSVERSE ELEMENTS ON THE PULLOUT CAPACITY OF METAL STRIP REINFORCEMENT IN SANDY SOIL**

## **ABSTRACT**

Interface friction angle between different materials is a very important parameter in the designs of mechanically stabilized earth (MSE) as it corresponds directly to pull out capacity of a reinforcement strip. In this research, anchorage elements have been added to normal reinforcement strip in order to increase interface friction angle and thus the pull out capacity. Sand was used as fill material. In the tests, one plain strip with smooth surface, two strips with simple ribs, and eighteen strips with transverse members of various depths and counts were subjected to pull out forces with normal stresses ranging from 50 kPa to 100 kPa applied. Also,  $\pi$ -Buchingham theorem and regression analysis using statistical software - SPSS v.14 - were used to obtain general equations relating pull out capacity to strip parameters and compare predicted strength values to actual outcomes of the tests. The results of the study indicate that the new method involving transverse members could generally offer saving of strip material or provide particular design criteria for MSE of limited construction space, since the increased capacity of each reinforcement strip would reduce the total length or amount of strips required in a project. Also in this research, direct shear apparatus used for soil testing was employed to measure the interface

shear resistance between well graded sand samples and galvanized steel plates. Finally, finite element computer modelling with Plaxis V 8.2 software was carried out to complete the analyses. The results from pull out tests combined with results from the modelling were found to be very useful for engineers to design better reinforced earth structures.



## **CHAPTER 1 INTRODUCTION**

### **1.1 Introduction**

Since the first installation of MSE by Vidal in 1961, the structure which is also known as either reinforced retaining wall, reinforced embankment, or reinforced soil, depending on the application, has been widely used in geotechnical projects where it provides a low-strain, strong, and durable solution for stabilization of fill or original material of the site (Bergado et al., 1987). Reinforced earth (Gurung, 2001) is made by reinforcing the soil with tension member like bar, steel plate, galvanized stripes, and geo-membranes. Reinforcement materials are categorized as either extensible such as the geotextiles and the geogrids or inextensible such as the metal strips and the metal grids; tests and analyses have been carried out involving both ( Ochiai et al.,1996; Khedkar and Mandal, 2009 and Balunaini and Prezzi, 2010). Interface friction angles between reinforcement materials and soils have been determined, the effects of various geometrical arrangements have been evaluated, and efforts have been made at having the reinforcement strips shortened while maintaining the required pull capacity such as by having the strips corrugated instead of plain (Potyondy, 1961; Zhang et al., 2008; and Racana et al., 2003).

Design of the MSE wall component of an MSE wall system should consider:

- Internal stability of the reinforced soil mass with regard to rupture and pullout of reinforcing elements such as pullout rupture of reinforcement and interface friction angle.
- External stability along the MSE wall/shoring wall interface such as friction between soil and MSE wall.
- Bearing capacity and settlement of the MSE wall foundation materials.
- Global stability of the composite SMSE wall system.

Generally speaking, the generic term ‘reinforced earth’ or ‘reinforced soil’ is used to describe all types of earth structures strengthened by reinforcements. However, in the industry, a large majority of reinforced earths has come under the more formal name category known as the mechanically stabilized earth or in short, MSE. Henry Vidal has been said as the inventor of the MSE (Haeri et al., 2000). Since the first installation of MSE by Vidal in 1961, the structure which also refers to reinforced retaining wall, reinforced embankment, and reinforced soil, depending on the application, has been widely used in geotechnical projects where it provides a low-strain, strong, and durable solution for stabilization of fill or original material of the site. In a MSE structure, reinforcement strips which are either metallic or synthetic, and plain or ribbed, are placed horizontally in the midst of layers of granular soil that is normally used as backfill or embankment material. Recent experiments and experiences involving MSE have been reported by many researchers (Varuso et al., 2005; Bathurst et al., 2005; Skinner and Rowe 2005; Hufenus et al., 2006; Nouri et al., 2006; Chen et al., 2007; Bergado and

Teerawattanasuk, 2008; Li and Rowe, 2008; Sieira et al., 2009; Palmeira, 2009; Abdelouhab et al., 2010).

Figure 1.1 is profile of a MSE as commonly installed today for road embankments where they apply. Inside the failure wedge, the reinforcement improves tension weaknesses in the soils, while across the potential slip surface, in the adjacent anchoring ground, the reinforcement holds the wedge against sliding or translational failure by having strips extended into the ground. For getting design parameters, pull-out tests are normally carried out. The pullout mechanisms of various reinforcement strips have been investigated not only by full-scale and laboratory model tests, but also by numerical methods (Palmeira and Milligan, 1989; Alagiyawanna et al., 2001; Gurung, 2001; Moraci and Cardile, 2009; Abdi and Arjomand, 2011; Goodhue et al., 2001; Sugimoto, 2003; Desai and Hoseiny, 2005; Moraci and Gioffre', 2006; Subaida et al., 2008; Su et al., 2008; Yin et al., 2008; Abdi et al., 2009; Zhou et al., 2011; Moraci and Cardile, 2012).

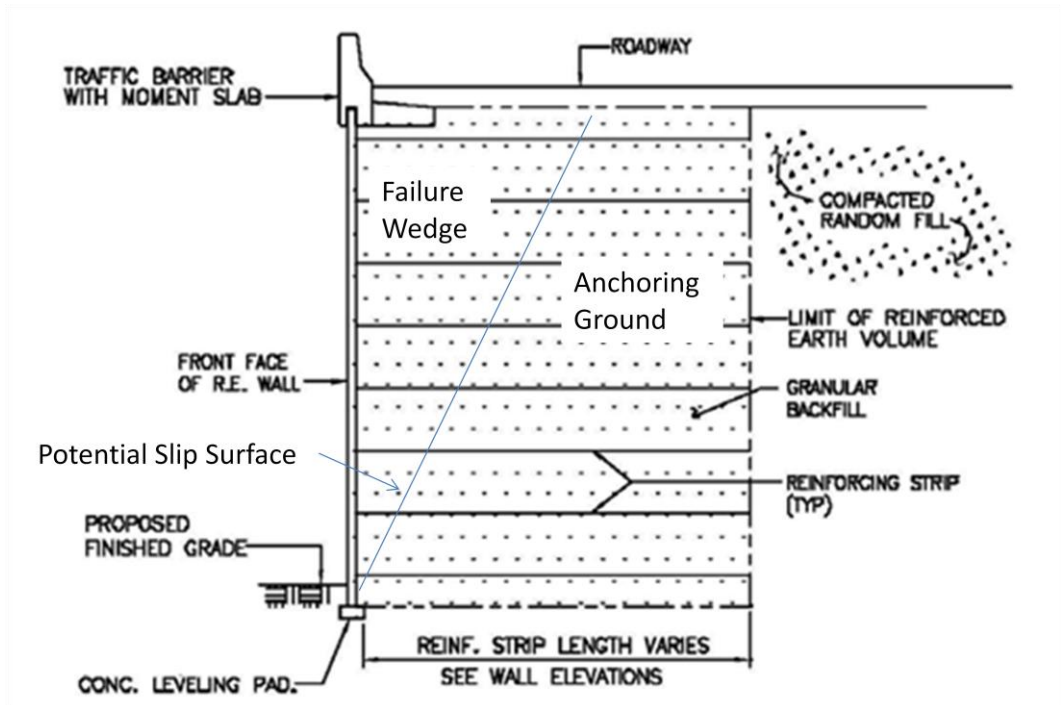


Figure 1.1: A profile of a commonly installed mechanically reinforced earth.(Sawicki, 2000)

## 1.2 Applications in Malaysia and abroad

The application of reinforced soil went back to ancient time, but since 1966 the method has been reinvented for design of reinforced retaining wall (Shukla et al., 2009). In the international arena of modern times, the use of reinforced retaining wall intensified in the 1980s and 1990s (Walls, 2009). In Malaysia, where soil reinforcement methods have been widely used in geotechnical projects, the use of reinforced earth for various geotechnical structures has become very popular in recent years. They can provide a low-strain, strong, and durable solutions for the stabilization of soils. From the front, outside of the reinforcement volume, view like shown in Figure 1.2 has become common sights in the country.



Figure 1.2: A view of MSE from the front showing decorative facing.

Inside the reinforcement volume, the interface friction angle between different materials is a very important factor in the design. The interface frictions between sand and galvanized steel is less than those between sand and sand because of the smooth surface of galvanized steel. Potyondy and Eng (1961) used smooth and rough materials, such as steel, wood, and concrete, to determine the interface friction between soil and these materials, restricting the moisture content and different normal loads between material and soil to find the interface friction of surfaces. The roughness of the steel, grain size of SW, and type of SW has been found to have an important effect on friction between two materials (Vesugi and kishida, 1981). Kishida et al. (1987) conducted some tests on the sand–steel interface using a simple apparatus and compared the results with those using others conventional apparatuses, such as direct shear test, annular shear test, and ring torsion experimental on the sand–plates interface; they compared the final results with those of other

experiments. The hardness of a material is the amount of surface resistance to the permanent indentation and may be considered a measure of the material strength. Hardness depends on both the geometry of the indenter and the material properties, including yield stress and bulk modulus. Moreover, it is not a true material property but rather a measurement. All materials with a low hardness amount have a high interface friction angle (Frost et al., 2002). Zhang et al. conducted a triaxial test to evaluate the interaction of horizontal-vertical orthogonal elements with sand and compared it with the ordinary horizontal type (Zhang et.al, 2008).

### **1.3 Recent trends in the use of geosynthetics**

The recent development in the industry has found increased use of geosynthetics – geomembrane, geotextile, geogrids – in replacing more traditional reinforcements made of metal strips, timbers, and geofabrics.

When geomembrane is used, soil interface parameter ( $\delta$ ) and shear strength of a smooth geomembrane–soil interface are discussed as in many studies by different researchers. Interface testing procedures and their effects on measured interface strength parameters have been investigated by Takasumi et al. (1991) and Fishman and Pal (1994). They gave a comprehensive review of the geomembrane–soil interface characteristics (Fleming et al., 2006).

When geotextile and geogrids are used, friction between soil and the geosynthetics materials facilitates the simple interface shear resistance of the soil against them - soil particles are not really engaged in the small space of the thin

geosynthetics sheet. However, the direct shear resistance is more complex for the thicker and more gripping geogrid. The wider ribs and soil contact enable greater interface shear resistance. At the same time, the friction resistance of soil particles on the top and bottom of the geogrid occurs within geogrid apertures. Therefore, the shear resistance of the soil–geogrid interface contains at least the shear resistance between soil and the surface of geogrids ribs and the internal shear resistance of the soil in the spaces of the geogrid. Interface between the granular fills and geogrid strip reinforcements in order to measure bearing resistance between the geogrid and soils have been studied by other researchers (Lin et al., 2005).

Yildize wasti et al., (2001) studied the subject by conducting the shearing test on PVC geomembranes, smooth and rough HDPE, nonwoven needle-punched geotextiles with 5–50 KPa range of normal stress, inclined board tests, and different sizes of interface surfaces. The length of reinforcement plate could be decreased by increasing the friction between the soil and reinforcement material, reducing the cost of soil reinforcing projects.

In future, with increased use in geogrid type of geosynthetics, but with thicker diameter threads, the knowledge on how resistance could be increased by having protrusions and shear elements is needed. In the study to be described next, the interface friction between sand and galvanized steel plate is increased by adding extra elements to the galvanized plate. The effect of different sizes and geometries of

shearing elements is evaluated using pull out tests, direct-shear tests, and Finite element modelling using Plaxis software.

#### **1.4 Problem Statement**

MSE has been widely used and the future is expected to see more usage including for narrow and complicated spaces where limitation of strips length is necessarily. Limitation on the use of strips is also caused by economy – the lesser the strips, the cheaper would the constructions be in terms of cost. However, with smaller number of strips used in an MSE, the force associated with a single strip becomes more, which in turn is affecting the mechanisms of tying the strip against the segmental concrete crust. In order to increase reinforcement capacity per strip, changing the geometry of the strip could be the solution.

In fact, the results of this study indicate that the new method involving transverse members could generally offer saving of strip material or provide particular design criteria for MSE of limited construction space, since the increased capacity of each reinforcement strip would reduce the total length or amount of strips required in a project. The test program described in this research was another attempt at having shorter or lesser number of strips involving inextensible material. The transverse members, also called anchorage elements, with element stiffeners, are part of a direct and simple means of improving anchorage through having rigid protrusions positioned 90 degrees to the direction of potential movement. The



expected outcomes were saving in strip material and new design criteria of MSE for narrow or limited construction spaces.

### **1.5 Objectives of the research**

1. To develop new strip for narrow place, with more pullout capacity and therefore economic benefits for projects.
2. To determine optimum depth of anchorage with given anchorage spaces or alternatively speaking, optimum anchorage distance for given anchorage depth.
3. To formulate pullout capacity for various given parameters based on pullout experimental results.
4. To study failure surfaces in soil reinforced with strips of various design and test conditions using finite element method (Plaxis software).

### **1.6 Scope of Research**

This research proposed to investigate the results to pull out capacity of strips with new geometries for mechanically stabilized earth, as would be applicable in walls in narrow or complicated spaces. Furthermore this research will utilise strips with different geometrise in pullout tests and carry out interface direct shear and direct pull out tests with different normal stresses. Statistical analysis and finite element modelling are needed to estimate final pull out strengths and investigate failure surface and behaviour of anchorage elements in the pullout tests.

## **1.7 Structure of Thesis**

This thesis is presented in five (5) chapters. First chapter introduces the research, objectives, problem statement, and scope. A review of previous study on pullout capacity and interface interactions, interface direct shear tests, past theories and experiments, and finite element methods are presented in Chapter 2. Chapter 3 presents research methodology implemented in this research. In chapter 4, results and discussion of tensile tests, pullout tests, interface direct shear tests, triaxial tests, and compaction tests are discussed. Finally the conclusion and recommendation for future work are presented in chapter five.

## **CHAPTER 2**

### **LITERATURE REVIEW**

#### **2.1 Introduction**

The research and industry of reinforced earth are generally more concerned with reinforcement material than with the earth fill material. The reinforcement materials, in turn, are comprised of steel and geosynthetics. The related tests carried out on these reinforcements are mainly the pull out tests and the direct shear tests. Computer modelling is carried out to corroborate the results. Pull out test and direct shear test are tow important experimental to investigate on soil and other material interface. For active zone of colomb failure surface and passive zone of MSE based on Mohr- colomb criteria direct shear test and pullout test are employed.

#### **2.2 Pull out and direct shear tests involving reinforcement material**

In study by Bakeer et al. (1998b), pull out test and interface shear test on geogrids were carried out against light aggregate with different confining pressures. In this study, the friction angles from pull out test was 52 degrees while from

interface friction test was 48 degrees, as given in Figure 2.1 and 2.2. Also, they found that some crushing actually had happened to the reinforced material with higher normal loads (Bakeer et al., 1998b).

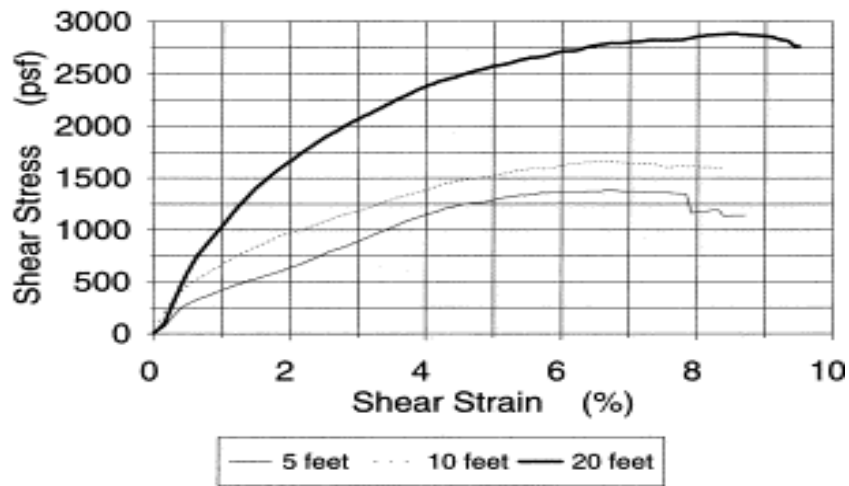


Figure 2.1: Results from pull out tests using geogrid and lightweight aggregate (Bakeer et al., 1998b)

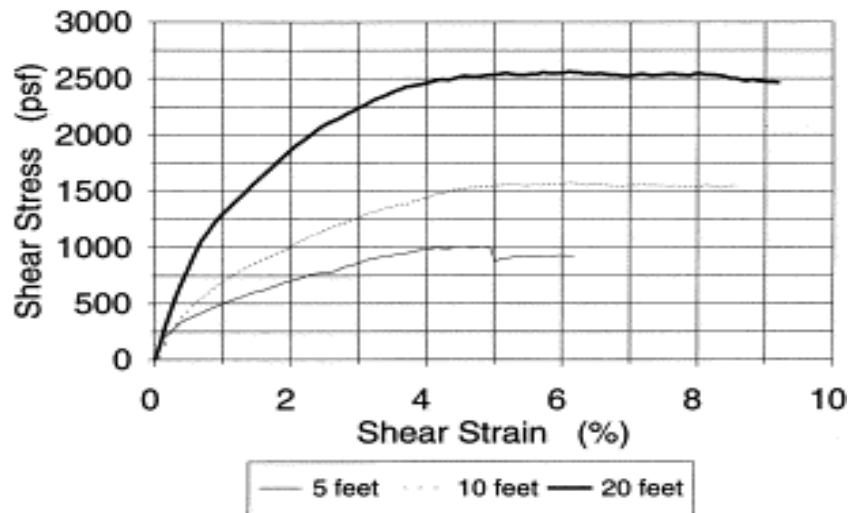


Figure 2.2: Results from interface shear tests using geogrid and lightweight aggregate (Bakeer et al., 1998b)

Boundary condition on pull out results was studied by Palmeira and Milligan (1989b). In this study, the results showed that certain friction on the inside of front wall of test box made it hard to predict the internal friction angle between soil and reinforcement material. They found that a larger scale pull out box and lubricating would be better in getting more accurate friction coefficient between materials.

In a study by Bergado et al. (1987), the interaction between soil and geogrids by using both direct shear and pull-out tests was investigated and the results were applied in a case study. Two types of Thailand soil - clayey sand and weathered clay – were used as backfill together with two types of reinforcement - polymer geogrid and bamboo grids. They found that the strength between soil and reinforcement has come from two factors: (a) the adhesion between soil and reinforcement on the solid surface area of the geogrid; and (b) the bearing withstand of soil in the fronts of the transverse members of geogrid that acted as a strip footing embedded in the soil. The design procedure for pull-out resistance coincided really well with the laboratory pull-out test results. Also their results showed that bamboo grids had higher pull-out resistance per unit area than the polymer geogrids. Furthermore, cohesive fills were found to be totally effective when used with geogrid reinforcement. Towards the end of their study, the results were applied in a design procedure to a case study involving an irrigation canal bank being repaired by the Public Works in Thailand. With Tensar SS2 geogrids as reinforcement and cohesive soils as backfill, a much improved embankment with very satisfactory slope stability was achieved.

Wilson Fahmy et al. (1994) carried out an investigations involving extensible reinforcement and dense sand in a series of pull out tests. They found that failures could take place by either sheet pull out or tension failure in the fill material. They have suggested that a great portion of pull out capacity was provided by the transverse elements thus the role of junctions in the reinforcement grids was very important. Also, the flexural capacity of traverse elements and the longitudinal extensibility of reinforcement should be considered as the main factor affecting the design involving this type of reinforcement.

A series of pull out tests have been carried out on extensible reinforcement and cohesion less soil by Oostveen et al. (1994). The results emphasized that front wall proximity was an important factor for the type of stress distribution on reinforcement - as suggested earlier by Palemira amd Miligan (1989).

Geogrids with various specifications and lengths were used in pull out tests by Frsman and Slunga (1994) in crushed rock, light clay aggregate, and sand material. Their results showed that, in a pull out test, when length of strips was increased, the average shear resistance was decreased because of progressive failure along the length of geogrid. With longer strip length, the lesser rigid would be the strip parts. Their results emphasized the roles of various factors such as strength of junction, rigidity of transverse bearing members, reinforcement strength, and modulus of deformation, on the pull out-displacement relationship.

According to Gurung and Iwao (1999), pull-out tests are widely employed to measure the soil-reinforcement interface interaction mechanism. They founded a simplified analysis for evaluation of the interaction mechanism in a general pull-out test which is proposed for geo-reinforcement. They also have done numerical studies for pull-out tests of different strains (large and small) for each type of inextensible to extensible reinforcements. They also have made comparison between the steel geostrap and polymer strip to verify the theories on both extensible and inextensible reinforcements. These researches have produced experimental and theoretical pull-out test results for various materials such as geotextiles, polymers, nylon geosynthetics and steel strip reinforcements. The predictions of pull out capacities were based from the models and their satisfactory comparisons with experimental results. The incorporated bi-linear relation allowed prediction of pre and post yield deformations, tensile force, and shear stress variations along the required length of the reinforcement.

In general, reinforcements are categorized in two major types, inextensible and extensible. Galvanized metal strips (straps), rock bolt, steel grids are called inextensible while geosynthetics, fibres, and polymers are called extensible reinforcement according their large strains resulted in pull out tests, as shown in Figure 2.3 (Gurung, 2001).

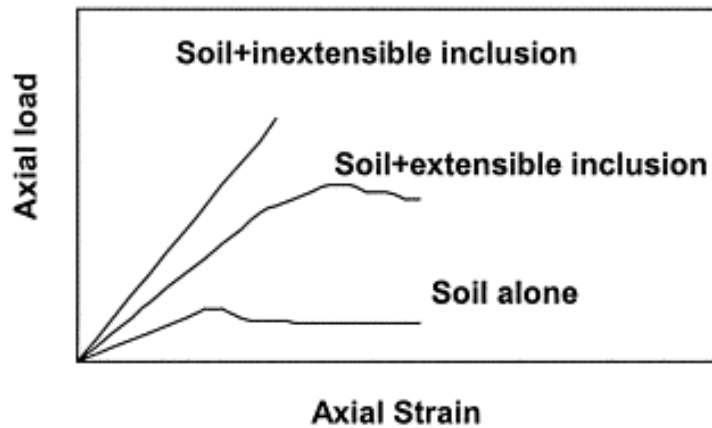


Figure 2.3: Description for inextensible and extensible reinforcements ( Gurung, 2001))

Alagiyawanna et al. (2001) carried out pull out tests using extensible geogrid with high strain of geometries as shown in Figure 2.4. Their results indicate that in case on extensible reinforcement, longitudinal members were more significant member in providing the required pull out capacity in comparison to the lateral bearing member during the failure phase of the geogrid. In this case, the large displacement of reinforcement will limit role of transverse members in providing the pull out capacity. Figure 2.5 depicts some results from pull out tests using feasible and rigid fronts.



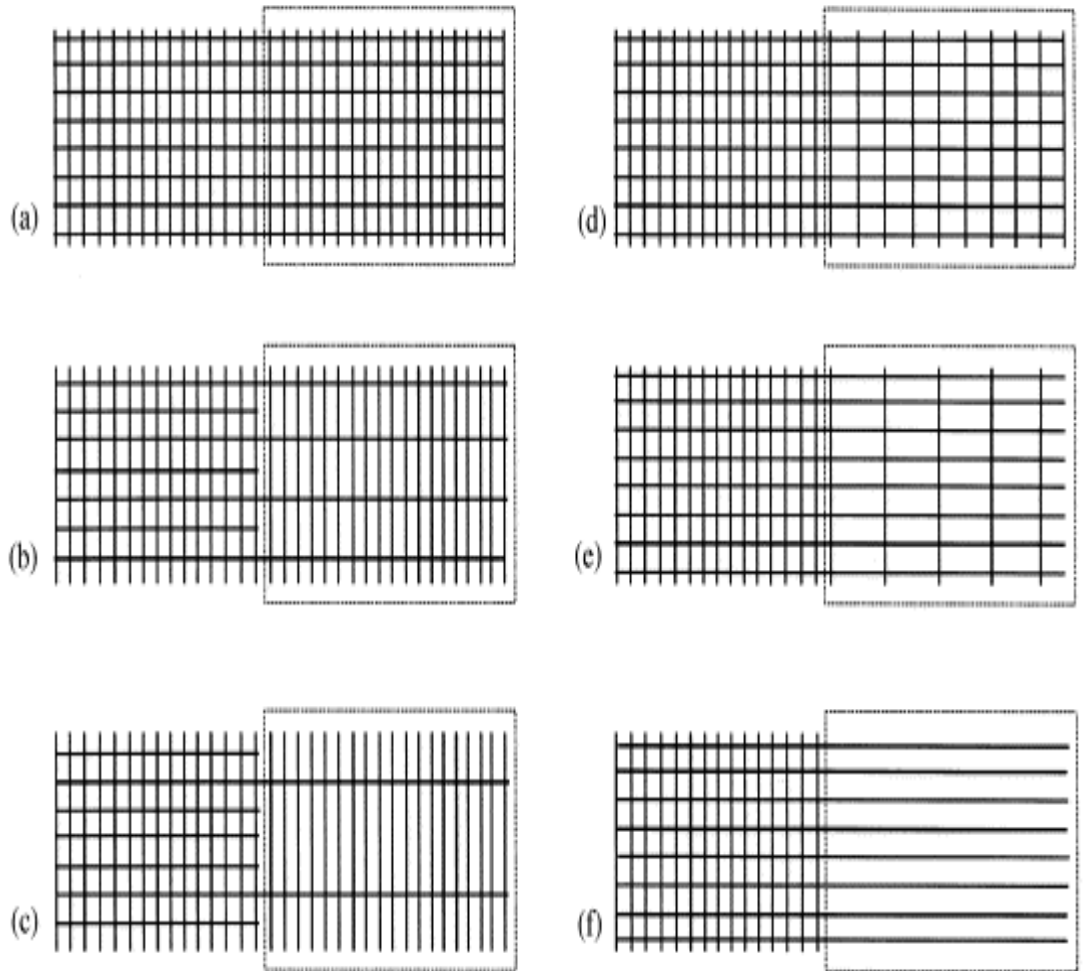


Figure 2.4: Geogrids used in pull out tests by Alagiyawanna et al., (2001)

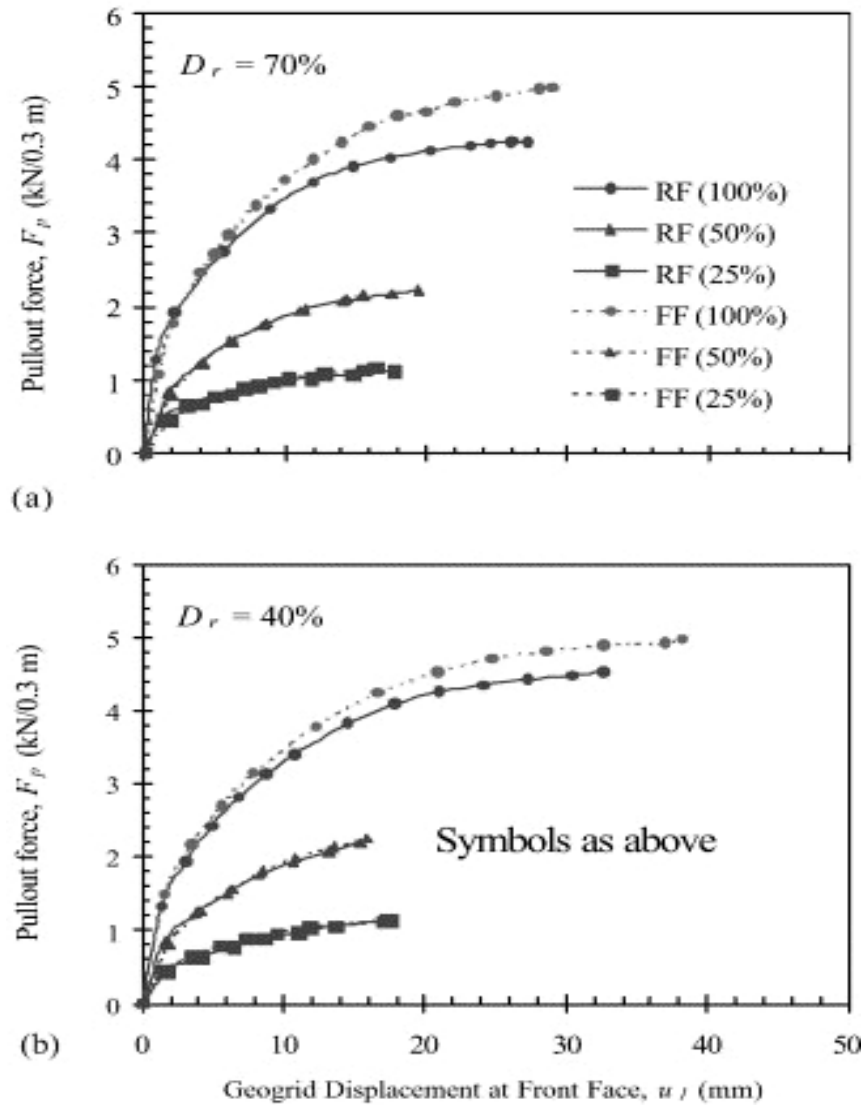


Figure 2.5: Results of pull out tests for flexible and rigid reinforcement members by Alagiyawanna et al. (2001)

Interface shear strength parameters of Geomembrane–geotextile were studied by Wasti and Bahadır Özdüzgün (2001) using 3 types of tests involving, the inclined board (tilting table), the standard sized direct shear box (60 mm×60 mm), and the large-scale direct shear box (300 mm×300 mm). HDPE, PVC geomembranes with Smooth and rough surfaces, and nonwoven needle-punched geotextiles were used in

the study. The inclined board tests were done under 5 to 50 kPa normal stresses on interface with various areas. The direct shear tests were conducted on normal stresses of 25 to 300 kPa for the smaller box and 110 to 400 kPa for the larger box. The results are given in Figure 2.6.

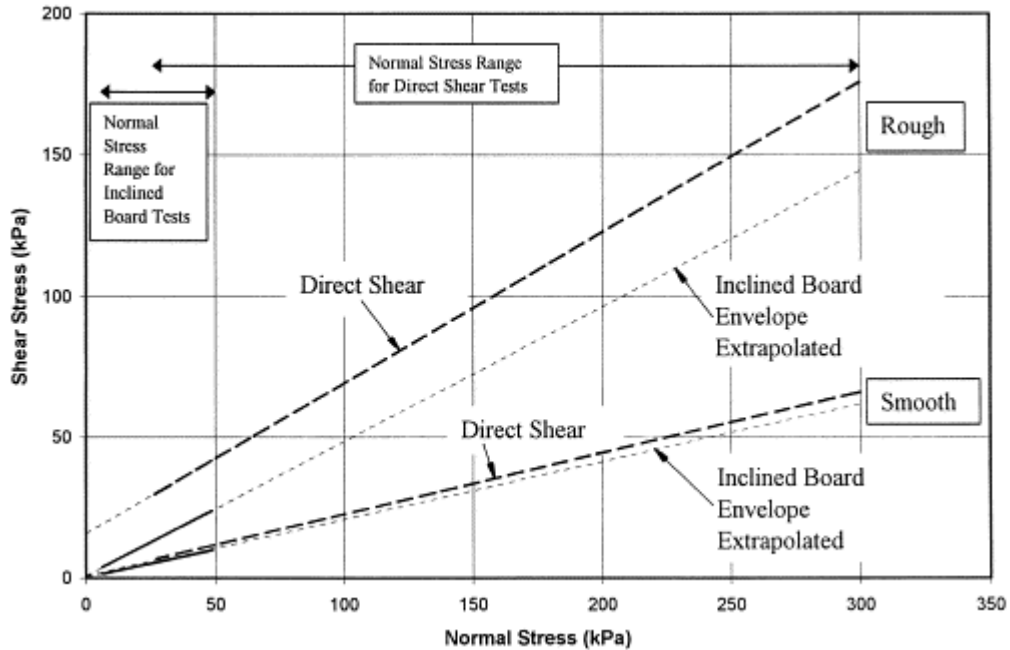


Figure 2.6: Results from inclined board test and large direct shear box tests involving 60 mm×60 mm geomembrane and geotextile interfaces (Wasti and Bahadır Özdüzgün, 2001)

The results with cohesion and interface friction angle values by fitting a straight line through the plots of interface shear strength versus the normal stresses were compared for different tests. They found that the inclined board test both smooth and rough HDPE geomembrane–geotextile interfaces had produced envelopes with small amount of adhesion. The interface size however was not significant factor. For smooth geomembranes, direct shear and inclined board tests both gave different interface friction angle and cohesion values. Their results showed

that the direct shear adhesion and friction values were markedly higher compared to those obtained from the inclined board tests, as given in table 2.1.

Table 2. 1: Different friction angle with different confining pressure (Wasti ,2001)

Interface	Giroud et al (1990) $\bar{\sigma}$ =1.1 kPa	Koubouras et al.(1991) $\bar{\sigma}$ =2.7 kPa	Girard et al.(1990) $\bar{\sigma}$ =3.7 kPa	Prescart study for $\bar{\sigma}$ =5or5.5 kPa	Giroud et al (1990) $\bar{\sigma}$ =25-160 kPa	Koubouras et al.(1991) $\bar{\sigma}$ =30-62 kPa	Girard et al.(1990) $\bar{\sigma}$ =100-400 kPa	Prescart study for $\bar{\sigma}$ =110-400 kPa
Smooth HDPE-GT	—	$\delta$ =19	—	$\delta$ =14-21		$\bar{\sigma}$ =2.8 kPa $\delta$ =10	—	$\bar{\sigma}$ =0.7-3.3 Kpa $\delta$ =12-14
Rough HDPE-GT	$\delta$ =45	$\delta$ =34	—	$\bar{\sigma}$ =33-42	$\bar{\sigma}$ =1.1 Kpa $\delta$ =15	$\bar{\sigma}$ =17.2 Kpa $\delta$ =15	—	$\bar{\sigma}$ =13-30 Kpa $\delta$ =13-30
PVC-GT	—	$\delta$ =22	$\delta$ =25	$\delta$ =23	—	$\bar{\sigma}$ =0 Kpa $\delta$ =26	$\bar{\sigma}$ =0 Kpa $\delta$ =34	$\bar{\sigma}$ =1-2 Kpa $\delta$ =24-25.5

Goodhue et al. (2001) conducted pull out test and direct shear test to find interaction coefficient ( $f$ ) between foundry sand, grids and geotextile, and textiles. Their results showed that interface friction angles had ranged from 25 to 35 degree, with efficiencies amounting to between 0.5 and 0.9. Also, the pull out tests results indicated that the interaction coefficient was varied from 0.2 to 1.7.

Racana et al. (2003), have done pull out tests on vertical, horizontal and corrugated strips of different geometries in order to validate their finite element

equations. They found that if the strain was low, more overall pull out capacity would be realized from the system. Their finite element formula also had 23% higher pull out capacity in comparison with the results from experimental study, as given in Figure 2.7 .

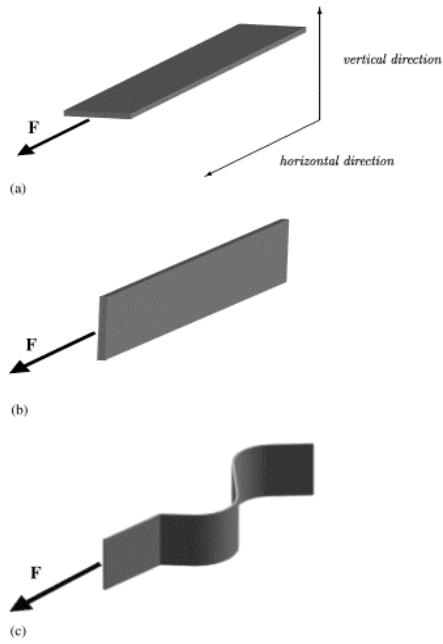


Figure 2.7: Strips of different geometries (Recana et al., 2003)

Numerical and experimental study further indicate that the low strain and overall increased pull out capacity in corrugated stripe was beneficial in the use smaller length of strips in practice as given in Figure 2.8, 2.9, and 2.10.

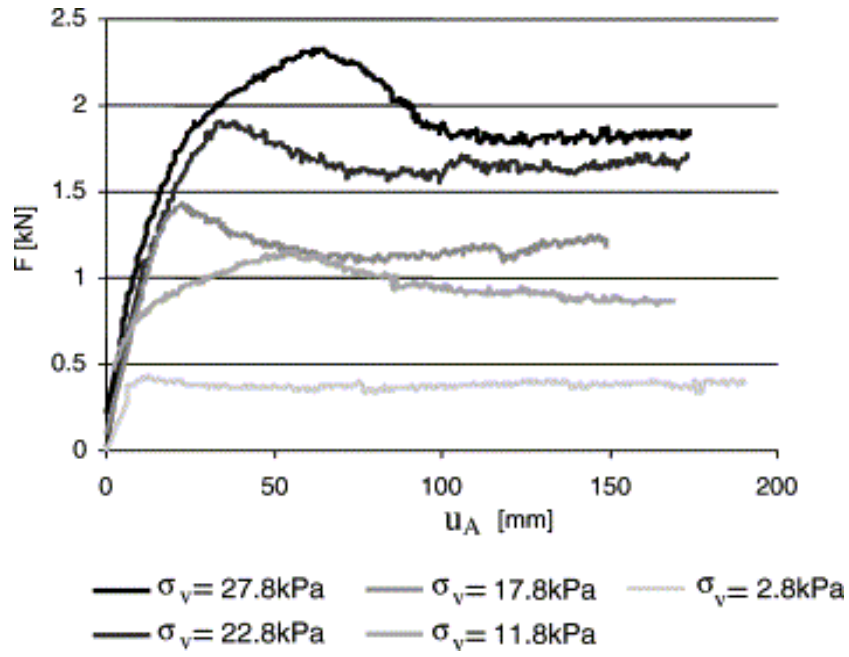


Figure 2.8: Pull out capacity for horizontal strips (Recana et al., 2003)

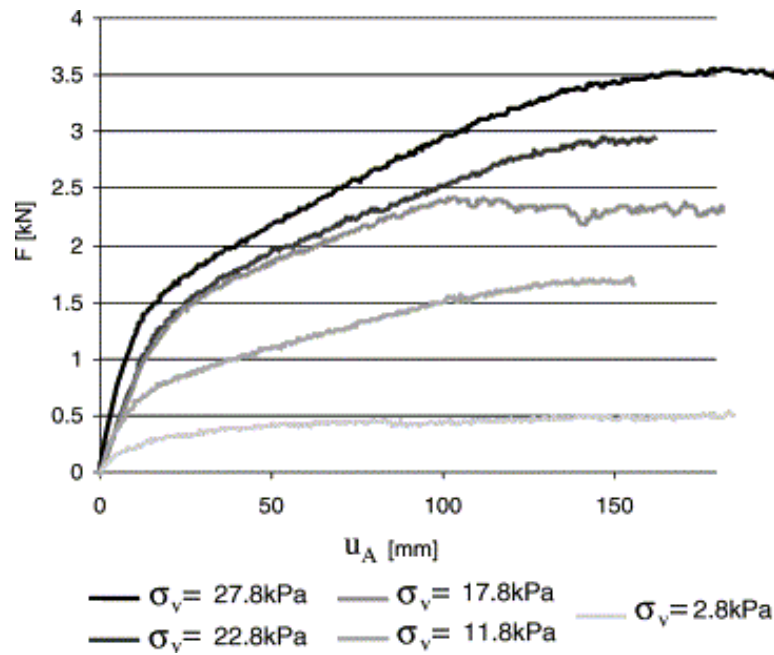


Figure 2.9: Pull out capacity for corrugated strip (Recana et al., 2003)

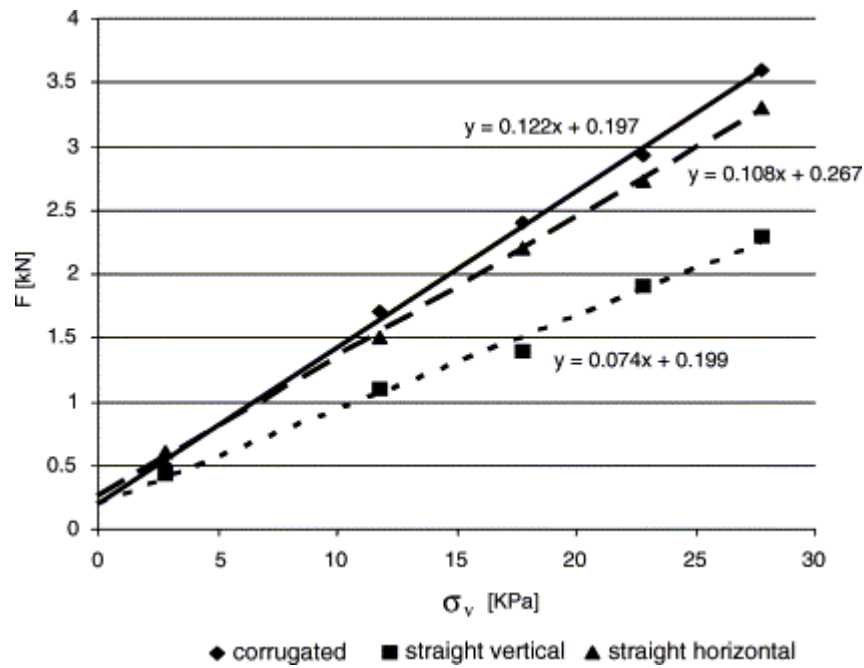


Figure 2.10: Pull out force for straight vertical, straight horizontal, and corrugated strip (Recana et al., 2003)

Palmeira (2004) studied on the mobilization of bearing forces in reinforcement during pull-out test. In this study, a theoretical model was made to describe the effects of having transverse ribs of geogrid in a large scale pull out test. Various mechanical and geometrical properties were tried with the model. Also investigated were the effects of some parameters such as free reinforcement length and test speed. He also found that good fill materials could make for shorter anchorage lengths in reinforced walls and slopes. He concluded that the length of reinforcement would affect overall stability of the reinforced mass, deformations, and final cost. Thus, the interaction between soil and geogrid is very important factor in the design of reinforce earth structure. Some results by Palmiera (2004) are given in Figure 2.11.

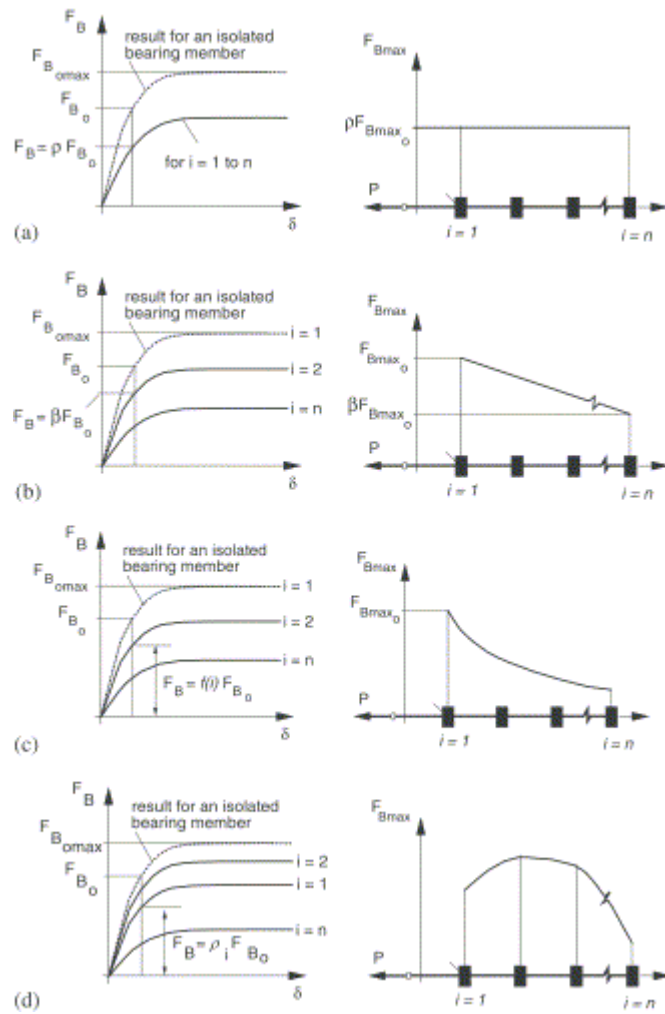


Figure 2.11: Cases of bearing strength degradation: (a) Reduction of uniform bearing force, (b) Reduction of linear bearing force along grid length, (c) reduction of bearing force as a power relation, (d) variable reduction of pull out force along the reinforcement (Palmeira, 2004)

Nejad and Smal (2005) conducted pull out test and direct shear test on geogrids and investigated interface and dilatancy angle and property in two types of soil. They have also compared the results with those coming from equations by Jewell et al. (1984) and Peterson et al. (1980). They results showed that the pull out tests showed higher amount of resistance than the direct shear tests – due to presence